Self-organized ensembles of nematic domains in magnetic and electric fields

Alexander M. Parshin [1,2,*] Victor Ya. Zyryanov [1] and Vasily F. Shabanov [1]
[1] *Kirensky Institute of Physics, Federal Research Center – Krasnoyarsk Scientific Center, Siberian Branch, Russian Academy of Sciences, Krasnoyarsk 660036, Russia*
[2] *Siberian Federal University, Krasnoyarsk 660041, Russia*

(Received 5 April 2022; revised 30 June 2022; accepted 28 July 2022; published 9 August 2022)

The structural and magneto- and electro-optical properties of a self-organized ensemble of nematic domains formed on a polycarbonate film in the presence of a residual solvent are studied. The film covered one of the plane-parallel glass plates of a liquid crystal cell. The magnetic field stabilizing the planar alignment of the liquid crystal was applied parallel to the cell surfaces and the reorienting electric field, perpendicular to them. The voltage dependences of the intensity of light transmitted through the domain ensemble were obtained at different constant values of the magnetic field. The comparison of the experimental dependences with the dependences calculated using the liquid crystal free-energy minimization procedure has shown good agreement between them. The mutual effect of structural elements of the ensemble and the effects of phase modulation of light are analyzed by comparing the structural, magnetic, and electric coherence lengths.

DOI: 10.1103/PhysRevE.106.024703

I. INTRODUCTION

At present, self-organized liquid crystal (LC) structures are being intensively studied and find wide application [1,2]. The formation of these structures is facilitated by the trend of LCs to molecular ordering. Even in the absence of a specific interaction with solid surfaces, nematic LCs form characteristic orientational structures that are observed in a polarizing microscope as threadlike or schlieren textures [2,3]. More complex nematic structures are formed in closed cylindrical or spherical volumes [3], e.g., in droplets of polymer-dispersed liquid crystals (PDLCs) [4,5]. By applying a magnetic [6,7] or electric [4] field to a PDLC, one can effectively control the light scattering and excite the phase modulation of light without polarizers, which is widely used in information display systems [4]. In addition, particular attention in both fundamental research and application is paid to the nematics in plane-parallel cells with the surfaces coated with light-activated substances, for example, azo dyes, in the form of single layers or polymer films [8]. Light irradiation of the coating evokes a planar-to-homeotropic anchoring transition or a change in the LC structure. When studying these processes, it is necessary to take into account the competition between the trans- and cis-configurations of a director [9], the correlation between the surface and bulk orientations [10], and the effect of the LC molecular structure on the photo-ordering process [11]. The competing factors promote the formation of patterns [12,13] that can be artificially created in local areas of an LC cell using polarized light [10,14,15] or an electric field of variable amplitude [16]. The patterns attract by a diversity of diffraction and interference effects [11].

Recently, we have found and briefly analyzed self-organizing patterns of nematic LCs on the polycarbonate (PC) surface [17–25]. Such patterns emerge spontaneously during the growth at the LC-polymer interface in the presence of a residual solvent. Over time, a self-organized ensemble of nematic domains (SEND) with disclination lines (DLs) appears in the LC layer. It was shown that the self-organization is caused by the physicochemical interaction of LC molecules with PC chains [17,19,21,22] under the competing impacts of a planar radial (PR) structure and DL over the coherence length ξ. These impacts are influenced by forces propagating from the coating surface of an LC cell processed to set oblique, planar, or homeotropic orientation. When light is passed through the SEND structure, attractive optical phenomena associated with interference, modulation, and light scattering are revealed. It was found that during the development of SEND, the light intensity is directly proportional to the radius of the domains due to the scattering of light by structural inhomogeneities [17,21,22]. In an electric or magnetic field, in the SEND cells, the interference oscillations with a much larger amplitude than in PDLCs and the light scattering effects were observed [18,21]. In [23,24], the electro- and magneto-optical studies of the SEND with good agreement between the calculated and experimental results were carried out using the magnetic ξ_H and electric ξ_E coherence lengths in the one-constant approximation [26].

However, the study of individual types of scattering in the process of domain growth as well as separate studies of the effects associated with interference due to LC birefringence and phase modulation of light are difficult under standard experimental conditions due to the presence of several competing factors in the LC cell, which allow simultaneous director deviation in azimuthal and polar orientation angles. Nevertheless, under such conditions, it is possible to apply a magnetic field in the cell plane, stabilizing the planar alignment [27]. This

*parshin@iph.krasn.ru

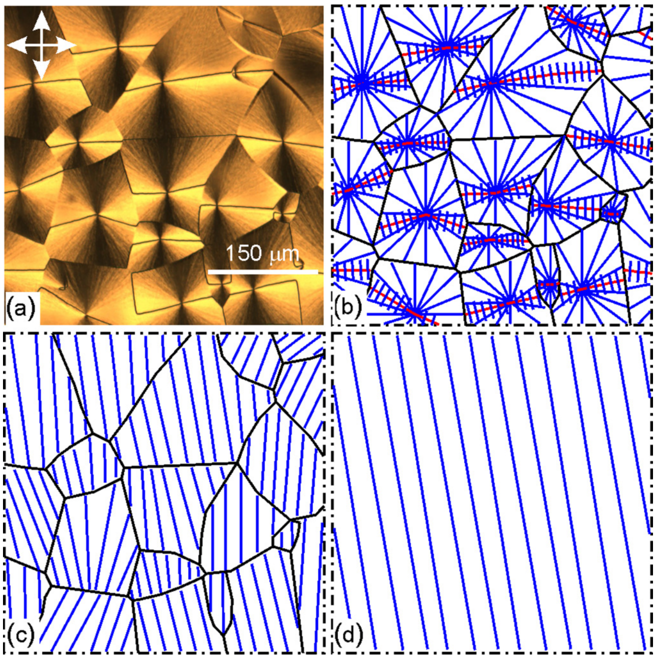

FIG. 1. Ensemble of 5CB domains formed on a PC film in the presence of a residual solvent: (a) texture observed between crossed microscope polarizers, (b) structure on the film surface at $z = 0$, (c) structure at the distance $z < \xi$, and (d) uniform alignment of an LC at $z > \xi$.

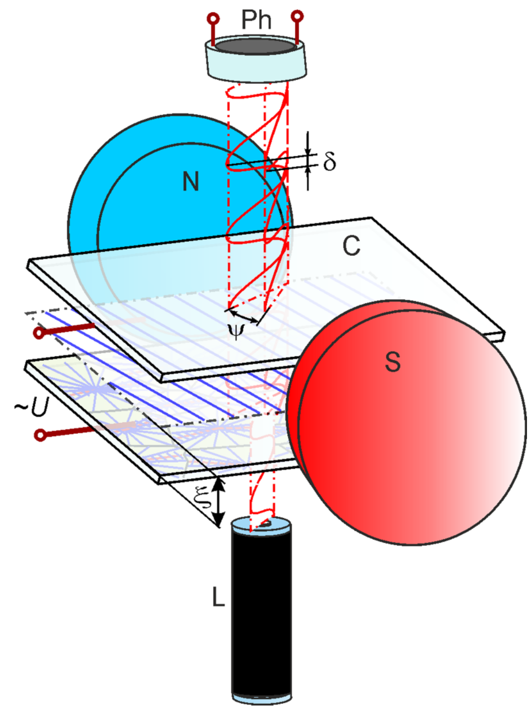

FIG. 2. Schematic of the propagation of laser radiation L through the SEND in cell C located between the N-S poles of an electromagnet. U is the voltage on the cell, d is the thickness of the LC layer, ξ is the structural coherence length, ψ is the angle between the polarization planes, and δ is the phase difference between the o and e waves, respectively.

field will allow one to eliminate polar deviations emanating from the cover surface, as well as to remove the azimuthal splitting of the director lines with a decrease in ξ_H.

The aim of this study was to investigate the structural and optical characteristics of the SEND using stabilizing magnetic and reorienting electric fields. The experimental and calculated dependences of light transmission on magnetic and electric fields were obtained and the structural, magnetic, and electric coherence lengths were compared.

II. STRUCTURAL AND OPTICAL PROPERTIES OF THE SEND

Let us briefly consider the formation of a SEND structure. In the presence of a residual solvent, nuclei emerge spontaneously on the PC film surface and evolve in disk-shaped nematic structures. The disk diameters increase uniformly within 120–1200 s, depending on the preparation conditions [21], and a close-packed ensemble of domains with the texture shown in Fig. 1(a) is formed in the bulk LC layer. DLs outgo from the centers of domains to their edges along the radii on opposite sides. The domain walls, which touch and cut off each other during the growth, outline the patterns that are well described by the Voronoi inverse tessellation algorithm [13]. The configuration of the domain ensemble on the PC surface is shown in Fig. 1(b). The lines of the director $\mathbf{n}_r$ develop the PR configuration from the domain centers. The DLs are sections of polymer chains (PCh); perpendicular to these sections, the nematic molecules are attached to the side chains. Most of the nematic molecules in the asymmetric configuration of the LC-PCh are rigidly attached to the surface due to adsorption, with the exception of a narrow homeotropic part that visualizes the PCh and reproduces a dark line in the middle along the DL in the optical pattern [17,19,21,22].

Each DL is located on PC film and forms a surface DL corresponding to the type that was topologically defined in Ref. [28]. According to the proposed definition, the DL strength $\Sigma = \Delta\theta/2\pi = 1/2$ at $\Delta\theta = \pi$ for the planar ordering of the LC. The LC molecules sequentially adjust to it with the formation of the director $\mathbf{n}_l$, which extends into the bulk over the structural coherence length ξ. At this length, the competition between the PR and DL orientations weakens and the nematic finds the lowest-free-energy state in a domain, which corresponds to the planar homogeneous orientation (HO) [Fig. 1(c)]. Domain walls are easily broken and a region covering many domains with the planar HO arises in the LC layer at the distance ξ [Fig. 1(d)]. Such a domain structure is pronounced in a droplet with the free upper boundary of the nematic layer or in a cell (Fig. 2) in which the LC layer is bounded by a glass surface facilitating the planar or oblique alignment of the director $\mathbf{n}$. By specifying weak anchoring [26] of an LC to the glass surface or a pretilt [29] and applying magnetic field H in the substrate plane, one can obtain the planar HO in the bulk of a cell at the length ξ_H from the PC film. Electric field E applied perpendicular to the cell surfaces will tend to establish the homeotropic orientation in the LC layer at the length ξ_E from the PC film. The equilibrium configuration of $\mathbf{n}$ can be determined by comparing the coherence lengths ξ, ξ_H, and ξ_E and finding the minimum free energy F of the nematic. We write the equation for F in the volume V of a domain in crossed magnetic and electric fields in the form

$$F = \frac{1}{2}\int_V \left\{ K[(\nabla\cdot\mathbf{n})^2 + (\nabla\times\mathbf{n})^2] - \Delta\chi(\mathbf{n}\cdot\mathbf{H})^2 - \frac{1}{4\pi}\Delta\varepsilon(\mathbf{n}\cdot\mathbf{E})^2 \right\} dV, \qquad (1)$$

where K is the elastic constant in the one-constant approximation and $\Delta\chi$ and $\Delta\varepsilon$ are the diamagnetic and dielectric anisotropy, respectively.

A conventional procedure for minimizing the nematic free energy after writing Eq. (1) in the cylindrical coordinates (x, y, z) with the substitution of the director components $\mathbf{n}_\rho = -\sin\theta$, $\mathbf{n}_\varphi = 0$, and $\mathbf{n}_z = \cos\theta$ into it (θ is the angle of deviation of $\mathbf{n}$ from the normal to the cell surfaces) yields

$$\nabla^2\theta = \left(\frac{A^2}{\xi^2} + \frac{1}{\xi_H^2} + \frac{1}{\xi_E^2}\right)\sin\theta\cos\theta, \qquad (2)$$

where $A = [(\pi^3/12 - \pi^2/4 + 1)/2\pi\ln(l/w)]^{1/2}$ [19], $l = \langle 2r\rangle$, w is DL width, r is the domain radius, $\xi_H = (1/H)(K/\Delta\chi)^{1/2}$ and $\xi_E = (1/E)(4\pi K/\Delta\varepsilon)^{1/2}$ [26] are the magnetic and electric coherence lengths, and $\nabla^2\theta = \partial^2\theta/\partial\rho^2 + (1/\rho)\partial\theta/\partial\rho + (1/\rho^2)\partial^2\theta/\partial\varphi^2 + \partial^2\theta/\partial z^2$ is the Laplacian. Assuming $\partial\theta/\partial\rho = 0$, $\partial^2\theta/\partial\varphi^2 = 0$ [19] and integrating, we arrive at

$$\left(\frac{d\theta}{dz}\right)^2 = \left(\frac{A^2}{\xi^2} + \frac{1}{\xi_H^2} + \frac{1}{\xi_E^2}\right)^{1/2}\sin^2\theta. \qquad (3)$$

The constant appearing during the integration is taken to be $C = 0$, since the PR configuration over the lengths ξ and ξ_H gradually turns into planar and, over the length ξ_E, into the homeotropic HO with $\theta = 0$ and $\partial\theta/\partial z = 0$.

In the optical context, we can consider small crystalline plates in a domain with local orientations of the director $\mathbf{n}_r$, with the average size r corresponding to the correlation radius of equilibrium fluctuations of the order parameter [23]. Each plate has a local optical axis directed along $\mathbf{n}_r$ [26]. A DL can be presented as a narrow single-crystal plate with the width b, length $l = 2r$, and the optical axis directed along $\mathbf{n}_l$. The HO on the upper base of a cylinder has the optical axis directed along $\mathbf{n}$. The light wave with electric field strength E propagating through the PR structure will divide into the ordinary $(o, \mathbf{E}_o)$ and extraordinary $(e, \mathbf{E}_e)$ components with refractive indices n_o and n_e when falling onto a crystal plate. In the investigated case of a uniaxial nematic medium, we assume n_o to be independent of angles φ and θ and n_e to be independent of angle φ and use it as the effective refractive index $n_{\rm eff} = n_e n_o/(n_e^2\cos^2\theta + n_o^2\sin^2\theta)^{1/2}$ [30]. A pair of the o and e waves with the orthogonal components $\mathbf{E}_{o1}$, $\mathbf{E}_{e1}$ and $\mathbf{E}_{o2}$, $\mathbf{E}_{e2}$ outgoes from crystalline plates 1 and 2 located on the PR structure. The waves with the nonorthogonal components $\mathbf{E}_{o1}$, $\mathbf{E}_{e2}$ or $\mathbf{E}_{o2}$, $\mathbf{E}_{e1}$ deviated due to the small-angle scattering interfere on a photodetector (Fig. 2). It should be noted that such a superposition of waves is due to the divergence of the lines of the director of the radial structure and would not take place with HO [23]. So, at the distance ξ, the interference effect vanishes since all the $\mathbf{E}_o$ and $\mathbf{E}_e$ components become orthogonal. For the squared amplitudes of the resulting field $\mathbf{E}_{12} = \mathbf{E}_{o1} + \mathbf{E}_{e2}$ or $\mathbf{E}_{21} = \mathbf{E}_{o2} + \mathbf{E}_{e1}$ in the domain cross section perpendicular to the wave vector $\mathbf{k}$ of the light wave, we can obtain [23–25]

$$E_{12}^2 = E_{o1}^2 + E_{e2} + 2E_{o1}E_{e2}\cos\psi\cos\delta_z,$$
$$E_{21}^2 = E_{o2}^2 + E_{e1}^2 + 2E_{o2}E_{e1}\cos\psi\cos\delta_z, \qquad (4)$$

where ψ is the angle between the polarization planes of the interfering o and e waves and δ_z is the phase difference between them. In the crossed magnetic and electric fields, the integral phase difference δ at wavelength λ in the LC layer with the thickness $\zeta = (\xi_H + \xi_E) \leqslant \xi$ caused by the coherence lengths ξ_H and ξ_E is determined as

$$\delta = \frac{2\pi}{\lambda}\int_0^\zeta [n_{\rm eff}(z) - n_o]dz. \qquad (5)$$

Substituting dz from Eq. (3) into Eq. (5), we obtain

$$\delta = \frac{2\pi n_0}{\lambda(A^2/\xi^2 + 1/\xi_H^2 + 1/\xi_E^2)} \times \int_0^{\pi/2}\left[\frac{n_e}{(n_e^2\cos^2\theta + n_o^2\sin^2\theta)^{1/2}} - 1\right]\frac{1}{\sin\theta}d\theta. \qquad (6)$$

Averaging the components in Eq. (4), i.e., $\langle E_{12}^2\rangle = \langle E_{o1}^2\rangle + \langle E_{e2}^2\rangle + 2\langle E_{o1}E_{e2}\rangle\langle\cos\psi\rangle\cos\delta_z$, $\langle E_{21}^2\rangle = \langle E_{o2}^2\rangle + \langle E_{e1}^2\rangle + 2\langle E_{o2}E_{e1}\rangle\langle\cos\psi\rangle\cos\delta_z$, allows us to introduce the intensities of interfering waves $I_1 = \langle E_{o1}^2\rangle + \langle E_{o2}^2\rangle$, $I_2 = \langle E_{e1}^2\rangle + \langle E_{e2}^2\rangle$ and the resulting intensity $I = \langle E_{12}^2\rangle + \langle E_{21}^2\rangle$ with interference term $J = 2[\langle E_{o1}E_{e2}\rangle + \langle E_{o2}E_{e1}\rangle]$. Averaging the $\langle\cos\psi\rangle$ from 0 to $\pi/2$, we get $2/\pi$ since the orthogonal components do not interfere. Assuming that the amplitudes of the o and e waves in the LC are equal, and considering an exponential term that takes into account scattering, we obtain the equation for the intensity of light transmitted through the SEND structure,

$$I = \frac{1}{2}I_0\left[1 + \frac{2}{\pi}\exp(-\alpha z)\cos\delta\right], \qquad (7)$$

where I_o is the intensity of light passed through the homeotropic LC layer and α is the coefficient characterizing the attenuation of a light beam due to scattering.

III. EXPERIMENT

An LC cell was designed from two glass plates 10×15 mm in size with indium-tin oxide (ITO) conductive coatings. For applying a voltage, copper conductors were soldered to the coatings at the plate edges. A polymer film was deposited onto the lower plate from a 2% solution of PC in CH_2Cl_2 in a centrifuge. Two 30-μm-thick polytetrafluoroethylene (PTFE) spacers were placed on the film and an upper glass plate washed in boiling acetone and hexane was placed on top of them. The plates were glued together with epoxy resin and the obtained LC cell was installed in a 12-mm gap between the electromagnet poles. The cell was fixed so that the magnetic field H was parallel to the plates and the electric field E induced by the voltage U applied to the conductors was perpendicular to them. The vertical He–Ne laser beam was attenuated by a light filter and directed to a photodiode through the cell center perpendicular to the plates. The cell was filled with the 4-n-pentyl-4′-cyanobiphenyl (5CB) LC

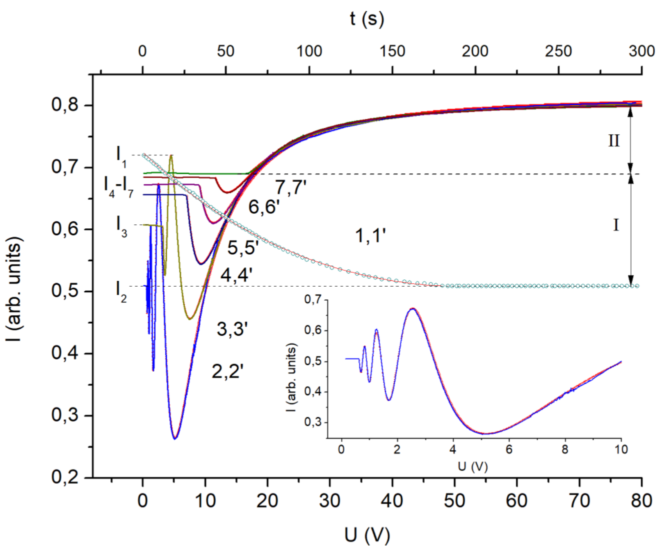

FIG. 3. Experimental (1–7) and calculated (1′–7′) dependences on light intensity I on time t and voltage U obtained in the processes of the SEND formation I_1–I_2 (the left-hand and upper axes) and LC reorientation I_2–I_7 under the action of voltage U in magnetic fields of H= (0, 0.4, 0.8, 1.2, 1.6, 2.15)×10^6 Am^{-1} (the left-hand and lower axes). Inset: initial part of the $I(U)$ dependence at $H = 0$.

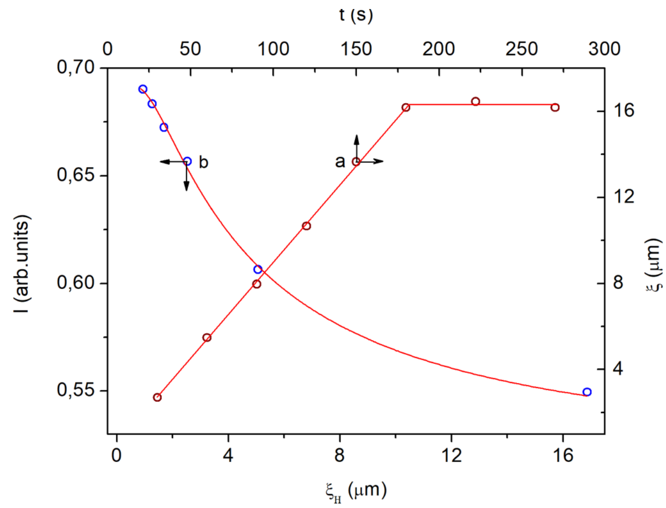

FIG. 4. Dependences of "a" the structural coherence lengths ξ on time t during the domain growth (the right-hand and upper axes) and "b" of the initial values I_2–I_7 of the light intensity I without voltage U on the magnetic coherent length ξ_H (the left-hand and lower axes).

in the nematic phase. The development of the SEND structure was monitored by a change in the laser radiation intensity. The magnetic field strength was fixed at a certain value in the range of $H = (0–2.15) \times 10^6$ Am^{-1}. At each fixed H value, the voltage with a frequency of 1 kHz from the generator was scanned at a rate of 0.07 Vs^{-1} in the range of $U = 0–80$ V. The light intensity values were detected with and without the empty and filled LC cell in the optical path. Upon completion of the experiment, the SEND texture was observed with a polarizing microscope and photographed [Fig. 1(a)]. All the procedures were carried out at 23 °C.

IV. RESULTS AND DISCUSSION

In Fig. 3, experimental curve 1 shows a decrease in the light intensity I from the instant of time $t_1 = 0\,(I = I_1)$ of the beginning of the domain growth to the time $t_2 \approx 180$ s $(I = I_2)$ of the completion of the SEND structure formation. This decrease is exponential and well described by the expression $I = I^* \exp{(a + bt + ct^2)}$, where I^* is the intensity of light passed through the empty cell. For simplicity, the I values were normalized to $I^* = 1$ and, using the exponential fitting, the coefficients $a = -0.321$, $b = -3.652 \times 10^{-3}$ s^{-1}, $c = 9.367 \times 10^{-6}$ s^{-2} at which curve 1′ coincides with good accuracy with curve 1 were obtained. We believe that the coincidence of dependences is not by chance since the propagation of light through a scattering medium is determined by probabilistic laws and the attenuation of the light flow occurs exponentially. Three terms in the considered expression can be related to different independent contributions of separate structural elements of the SEND to the scattering. In this case, the quantity I is the probability of light passage through the LC layer without scattering, which represents a product of the transmission probabilities of the elements. Other fitting functions such as polynomial, sigmoidal, or exponential without a quadratic term give poorer results. At the same time, we found a coincidence only in the interval of $0 < t < 180$ s and not in the entire time range $t \to \infty$. Apparently, this is due to the fact that up to $t_m = 180$ s the radius of the domains and $\xi = Ar$ increase in proportion to t, and above t_m the domains are deformed, but ξ remains constant, and only the shape of domains changes (Fig. 1). Part of curve 1 is approximated by a straight line. It should be noted that the coefficients a and b in the expression are negative and characterize the darkening of the LC layer, while the coefficient c is positive, which means the presence in the SEND structure of an element that contributes to the transparency of the structure.

At $t = 0$, the quantity I has a value of $I_1 = 0.725$ obtained for an LC layer with the threadlike texture. A decrease in the intensity I^*/I_1 by a factor of ≈1.4 results from the scattering by director fluctuations [26] and inhomogeneities of the misoriented LC layer [31]. The scattering of these types is characterized by the empirical coefficient $a = -0.321$.

The second term in the expression depends linearly on t and is related to the development of domains. Taking into account the effective scattering cross section σ', we can write this term as $I_1' = I^* \exp{(-\alpha' z)}$, in which $\alpha' = N'\sigma'$, with N' the number density of domains and σ' the scattering cross section, The $\alpha' = f(z)$ varies from α_0 exponentially over the length ξ by law $\alpha' = \alpha_0 \exp{(-z/\xi)}$. Since the z coordinate is limited in transition layer ξ of the structural transformation PR-HO during the growth of domains, it is reasonable to replace $z \to \xi$, $\xi \to \xi_m$, bringing these parameters into agreement with Fig. 4(a). The macroscopic scattering cross section $\alpha'(\xi)$ can be found by integrating $\alpha_0 \exp{(-\xi/\xi_m)}$ over ξ in the range from 0 to ξ_m and obtaining $\alpha' = \alpha_0 \xi(1 - 1/e)$. Since ξ_m is determined by the size of the domains, it can be represented as an efficient free path length for a light wave on structural inhomogeneities of SEND, and in that case, $\alpha_0 = 1/\xi_m$ should be used. From Fig. 4(a), it follows that $\xi = kt$, $k = 0.09$ μms^{-1}, and the second parameter of the term

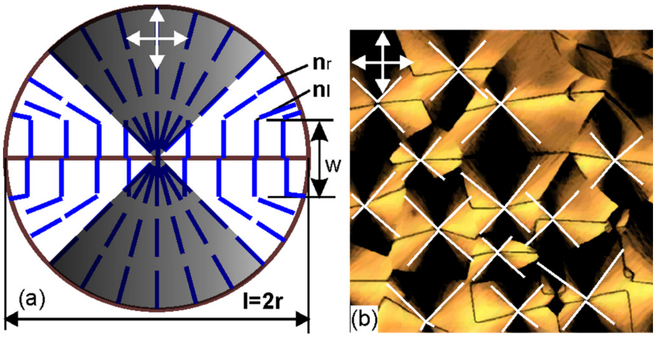

FIG. 5. LC domains on the PC film. (a) View of an individual growing domain between crossed microscope polarizers and domain structure; $\mathbf{n}_r$ and $\mathbf{n}_l$ are the director lines in the PR configuration, r is the domain radius, and w is the DL width. (b) Texture of an ensemble of domains with sharp walls.

in the expression for I is defined as $b = (k/\xi_m)(1 - 1/e) = 3.52 \times 10^{-3}$ s^{-1} in approximate agreement with the fitting value.

It should be noted that the light scattering occurs not on the entire domain, but only on its areas that are observed between crossed polarizers as bright sectors in the texture [Fig. 5(a)], where the vectors $\mathbf{n}_r$ and $\mathbf{n}_l$ corresponding to the director $\mathbf{n}$ on the PR structure and DL significantly diverge. As can be seen in Fig. 5(b), which is a high-contrast copy of Fig. 1(a), the areas of the bright and dark sectors are equal since their boundaries intersect at right angles. In addition, the domain is nonuniform and passes exponentially from the strongly scattering PR structure to the weakly scattering planar HO over the length ξ.

The third term in the expression for I depends quadratically on t and is related to the development of disclinations. The contribution of disclinations to the optical transmission can be expressed through the intensity $I_1'' = I^* \exp(\alpha'' z)$, in which $\alpha'' = N''\sigma''$, where N'' is the number of DL per unit volume. The scattering cross section $\sigma'' = f(t)$ with $z =$ const varies with time during the growth of domains and tends to set the HO over the length ξ, thereby promoting the brightening. According to Fig. 1(a), one DL is located on the PC area σ_0 occupied by one domain, and therefore, at a unit length $z = 1\,\mu$m, the value $N'' = 1/\sigma_0$. Herewith, DL increases the light intensity in the scattering part of the domain [Fig. 5(a)], the area of which, according to Fig. 5(b), is equal to $\sigma_0 = (1/2)\pi r^2$. The value of $\sigma'' = wl$, where w is the width and $l = 2r$ is the length of DL. It follows from experimental observations that the parameters w and l increase linearly with the growth of domains $w = k_w t$ and $l = k_l t$, $\sigma'' = k_w k_l t^2$. In the formed domain $k_w = w_m/t_m$, $k_l = l_m/t_m$, where $w_m = 10\,\mu$m, $l = 2r = 96\,\mu$m, $t_m = 180$ s. Relating the areas σ'' and σ_0, we obtain $\alpha'' = ct^2$, where $c = k_w k_l/\sigma_0 = 8.2 \times 10^{-6}$ s^{-2}, in approximate agreement with the fitting value.

The magnetic field H applied to the SEND in the PC film plane straightens lines of the director $\mathbf{n}_r$ in domains and establishes the planar HO at the distance $z \geqslant \xi_H$. As the H value increases, the LC cell brightens since the thickness of the scattering nematic layer limited by ξ_H decreases. It can be seen in Fig. 3 that for each higher H value, the initial intensities I_2–I_7 become higher. The voltage U applied at different H values starts reorienting the LC and the $I(U)$ dependences are modified. At $H = 0$, the deviation of I begins at a threshold value of $U_0 = 0.5$ V. After leaving the subthreshold region, the $I(U)$ curve increases and undergoes a series of transverse oscillations, which have a significant amplitude and are caused by the phase modulation of light due to the interference of the o and e waves. At the high-U values, the voltage-contrast characteristic tends to the saturation voltage U_s at the intensity I_0 corresponding to the transmission of a homeotropic LC layer. With increasing field H, the U_0 value grows, the interference oscillation amplitudes decrease, and the monotonic course of the $I(U)$ curve to the saturation region is preserved. At $H = 2.15 \times 10^6$ Am^{-1}, the extrema disappear completely, determining the boundary where the $I(U)$ curve with the initial I_7 value goes from the modulation to saturation region. The initial intensity increases exponentially from I_2 to I_7 since the brightening is described by the equation $I = I_7 - I_2' \exp(-\xi_{Hm}/\xi_H)$, where I_{2m} and ξ_{Hm} are the amplitude I and ξ_H values in the transition region. Substituting values of $\xi_H = \infty$ at $H = 0$ and $I_2 = 0.51$ from Fig. 3, we obtain $I_2' = 0.182$, $\xi_{H_m} = 0.391$, and $I_7 = 0.692$. The $I(\xi_H)$ dependence calculated at such parameters agrees well with the experimental curve [Fig. 4(b)].

The experimental and calculated $I(U)$ dependences in Fig. 3 are also in good agreement. The calculated curves were obtained by substituting the phase difference δ calculated from Eq. (6) into Eq. (7) for the light intensity. In the calculation, we used the literature data $K = 6.21$ pN, $\Delta\chi = 0.97 \times 10^{-7}$, $\Delta\varepsilon = 13.8$ [32], $n_o = 1.5271$, and $n_e = 1.7103$ [33] at 23 °C and the experimental values $d = 35\,\mu$m, $r = 48\,\mu$m, $l = 96\,\mu$m, $w = 10\,\mu$m, $\xi = r[(\pi^3/12 - \pi^2/4 + 1)/2\pi \ln(l/w)]^{1/2} = 16.2\,\mu$m, and $A = 0.337$. In the calculation of δ, values of $H = (0, 0.4, 0.8, 1.2, 1.6, 2.15) \times 10^6$ Am^{-1} and $E = (0.014 - 2.3) \times 10^6$ V/m ($U = 0.5$–80 V) were specified for each H value used to determine the coherence lengths ξ_E and ξ_H. The solutions of Eq. (7) consistent with the experiment were obtained using the scattering cross section $\sigma = \zeta/\xi$. This consistency is due to the fact that the fields E and H applied to the SEND cause the reorientation of the nematic in domains and the establishment of the HO at the distance $z \geqslant \zeta$. As the E or H value increases, the LC cell brightens since the thickness of the scattering nematic layer limited by ζ decreases. Upon slow scanning of E, the equilibrium configuration of the director $\mathbf{n}$ corresponding to the minimum nematic free energy is established at each instant of time.

In each section perpendicular to the z axis, light passes through many crystalline plates of the PR structure transforming into the HO one with the formation of a random interference pattern (speckle) on the photodetector [Fig. 6(a)], which represents a superposition of the coherent o and e waves with the polarization planes inclined at the angle ψ (Fig. 2). The speckle has the effective refractive index n_{eff} and $\langle\cos\psi\rangle$ that are constant over the cross section and independent of the magnetic field. Therefore, as can be seen in Fig. 3, with an increase in H, the threshold U_0 values in the $I(U)$ dependences shift without changes in the phase modulation. The modulation occurs upon variation in the polar angle θ under the action of an electric field; as a result, the o and e waves propagating along the z axis at different velocities shift in

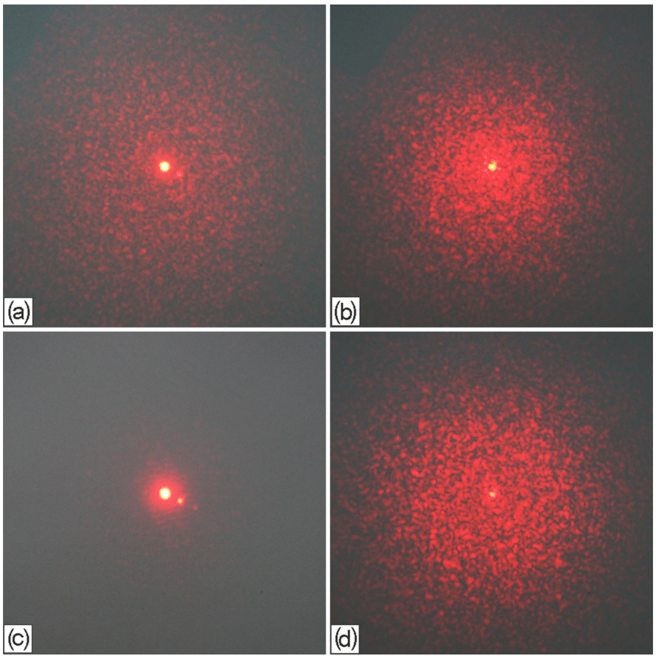

FIG. 6. Variation of the speckle arising during passage of laser radiation through the SEND under the action of a voltage of $U=$ (a) 0, (b) 2.5, (c) 5, and (d) 80 V.

phase by the δ value and interfere. Under these conditions, the interference is reflected on the photodetector as the speckle brightening and darkening (Fig. 6). It should be noted that the considered modulation occurs regardless of the polarization of the incident light and there is no need to use a polarizer in the optical path in Fig. 2.

V. CONCLUSIONS

We have studied the structure and optical properties of a self-organized ensemble of nematic domains during its formation and under the influence of crossed magnetic H and electric E fields. Domain ensembles were formed in a cell with the plane-parallel glass surfaces on a PC film during the growth in the presence of a residual solvent. The dependence of the light intensity on time during growth is obtained, and the scattering of light during the passage of laser radiation through the ensemble is estimated. We presented such scattering in the form of a probabilistic exponential function, which was expressed as a product of three independent events characterizing the scattering in the threadlike structure of the LC at inhomogeneities of sectors of the radial configuration and disclination lines, as well as at the boundaries of the disclination lines and domains.

We have estimated the change in the light intensity I as a function of the variation of the magnetic field applied parallel to the surfaces of the LC cell. This dependence is approximated by an exponential function whose argument is the magnetic coherence length ξ_H, which decreases exponentially from the surface. Good agreement between the calculated and experimental dependences $I(H)$ confirms the correctness of using ξ_H to estimate the change in I when the axial splitting of the radial configuration under the influence of a magnetic field is eliminated.

By minimizing the nematic free energy, the equations for the phase difference between the o and e waves and for the intensity I of the light transmitted through the investigated structure, influenced by crossed magnetic and electric fields E, were derived. Using the known parameters of the selected 5CB nematic, the $I(E)$ dependences at different H values were calculated. An LC cell was placed between the electromagnet poles and the magnetic field H was applied along the film. The voltage U was applied to the conductive ITO coatings deposited onto the glass surfaces of the cell to induce the electric field E perpendicular to the field H in the LC layer. The He–Ne laser beam propagated through the cell and was detected with a photodiode. The electric field was slowly scanned at different fixed H values and the experimental $I(E)$ dependence was built; the comparison of this dependence with the calculated one showed their good agreement. The structural ξ, magnetic ξ_H, and electric ξ_E coherence lengths were compared to estimate the mutual effect of structural elements of the self-organized ensemble.

The optical characteristics of the ensemble were explored, including the phase modulation of light observed without polarizers in the optical scheme and the scattering of light on different areas of the investigated structure. The use of a stabilizing magnetic field in the experiment made it possible to separately study the interference contributions to the intensity. It is shown that the interference of nonorthogonal ordinary and extraordinary waves gives a random interference pattern (speckle) due to the angle ψ characterizing the radial splitting. Light modulation is an interference variation of the speckle depending on the phase difference δ of the waves due to a change in the polar angle θ under the influence of an electric field. Such modulation does not require polarizers and can be effectively used for practical applications.

[1] A. Buka and L. Kramer, *Pattern Formation in Liquid Crystals* (Springer Verlag, New York, 1996).

[2] I. Dierking, *Textures of Liquid Crystal* (Wiley-VCN, Weinheim, Germany, 2003).

[3] M. Kleman and O. D. Lavrentovich, Philos. Mag. **86**, 4117 (2006).

[4] J. W. Doane, *Polymer Dispersed Liquid Crystals Displays: Liquid Crystals: Application and Uses*, edited by B. Bahadur (Word Scientific, Singapore, 1990), Chap. 14.

[5] O. O. Prishchepa, A. V. Shabanov, and V. Ya. Zyryanov, Phys. Rev. E **72**, 031712 (2005).

[6] O. O. Prishchepa, A. M. Parshin, A. V. Shabanov, and V. Ya. Zyryanov, Mol. Cryst. Liq. Cryst. **488**, 309 (2008).

[7] A. M. Parshin, V. G. Nazarov, V. Ya. Zyryanov, and V. F. Shabanov, Mol. Cryst. Liq. Cryst. **557**, 50 (2012).

[8] L. O. Palomares, J. A. Reyes, and I. Janossy, Phys. Rev. E **90**, 062503 (2014).

[9] T. Tóth-Katona and I. Jánossy, J. Mol. Liq. **285**, 323 (2019).

[10] I. Nys, Liq. Cryst. Today **29**, 65 (2020).

[11] A. R. K. Nassrah, I. Jánossy, and V. Kenderesi T. Tóth-Katona, Polymers **13**, 193 (2021).

[12] P. Ball, *Nature's Patterns* (Oxford University Press, Oxford, 2009).

[13] I. Dierking, A. Flatley, and D. Greenhalgh, J. Mol. Liq. **335**, 116553 (2021).

[14] I. Nys, J. Beeckman, and K. Neyts, Soft Matter **11**, 7802 (2015).

[15] Ya-Q. Lu, W. Hu, A. Srivastava, and V. Chigrinov, Proc. SPIE **8642**, 864201 (2013).

[16] T. Kósa, P. Coutino, A. Munoz, B. Taheri, and I. Janossy, Liq. Cryst. **46**, 145 (2019).

[17] A. M. Parshin, V. A. Gunyakov, V. Ya. Zyryanov, and V. F. Shabanov, Intl. J. Mol. Sci. **14**, 16303 (2013).

[18] A. M. Parshin, V. A. Gunyakov, V. Ya. Zyryanov, and V. F. Shabanov, Intl. J. Mol. Sci. **15**, 17838 (2014).

[19] A. M. Parshin, V. Ya. Zyryanov, and V. F. Shabanov, Liq. Cryst. **42**, 57 (2015).

[20] A. M. Parshin, V. Ya. Zyryanov, and V. F. Shabanov, Opt. Mater. Express **6**, 2841 (2016).

[21] A. M. Parshin, V. Ya. Zyryanov, and V. F. Shabanov, Sci. Rep. **7**, 3042 (2017).

[22] A. M. Parshin, V. Ya. Zyryanov, and V. F. Shabanov, Polym. Sci. Ser. C **60**, 23 (2018).

[23] A. M. Parshin, A. V. Barannik, V. Ya. Zyryanov, and V. F. Shabanov, J. Opt. Soc. Am. B **36**, 1845 (2019).

[24] A. M. Parshin, A. V. Barannik, V. Ya. Zyryanov, and V. F. Shabanov, J. Opt. Soc. Am. B **37**, 2053 (2020).

[25] A. M. Parshin, V. Ya. Zyryanov, and V. F. Shabanov, J. Opt. Soc. Am. B **38**, 2993 (2021).

[26] P. G. de Gennes and J. Prost, *The Physics of Liquid Crystals* (Clarendon, Oxford, UK, 1993).

[27] M. Glogarova and G. Durand, J. Phys. France **49**, 1575 (1988).

[28] V. Vitek and M. Kleman, J. Phys. **36**, 59 (1975).

[29] L. R. Evangelista, Phys. Lett. A **205**, 203 (1995).

[30] L. M. Blinov, *Structure and Properties of Liquid Crystals* (Springer, New York, 2010).

[31] L. M. Blinov and V. G. Chigrinov, *Electrooptic Effects in Liquid Crystal Materials* (Springer, New York, 1994).

[32] M. J. Bradshaw, E. P Raynes, J. D. Bunning, and T. E. Faber, J. Phys. France **46**, 1513 (1985).

[33] J. D. Bunning, D. A. Crellin, and T. F. Faber, Liq. Cryst. **1**, 37 (1986).